Heterogeneous & Homogeneous & Bio- & Nano-

CHEMCATCHEM

CATALYSIS

Accepted Article

Title: Morphology-tuned activity of Ru/Nb2O5 catalysts for ketones reductive amination

Authors: Wanjun Guo, Tao Tong, Xiaohui Liu, Yong Guo, and Yanqin Wang

To be cited as: *ChemCatChem* 10.1002/cctc.201900335

Link to VoR: http://dx.doi.org/10.1002/cctc.201900335

A Journal of ChemPubSoc Europe

WILEY-VCH

www.chemcatchem.org

10.1002/cctc.201900335

Morphology-tuned activity of Ru/Nb_2O_5 catalysts for ketones reductive amination

Wanjun Guo⊥[a], Tao Tong⊥[a], Xiaohui Liu[a], Yong Guo[a], Yanqin Wang*[a]

Abstract: Amines are important compounds in natural products and medicines. Specifically, cyclopentylamine is one of the value-added chemicals widely used in the production of pestisides, cosmetics and medicines. In this work, three Ru/Nb_2O_5 catalysts with different Nb_2O_5 morphologies were used in the reductive amination of cyclopentanone under mild reaction conditions (90 °C, 2 MPa H_2), among which 1%Ru/Nb_2O_5-L catalyst exhibits best performance with the yield of cyclopentylamine reaching 84%. This catalytic system is stable and has not significant deactivation even after 5 runs in the durability test. In addition, this catalyst can be extended to a series of aldehydes/ketones. Further comprehensive characterizations (XPS analysis and CO-adsorption DRIFT) reveal that the electronic effect of Ru species can be ruled out; instead, the activity of the catalyst is strongly influenced by the geometric effect. Layered Nb_2O_5 material possesses the highest surface area, resulting in the highest Ru dispersion, and therefore shows the highest catalytic activity. The in-situ DRIFT-MS technique was also used to reveal and understand the reaction mechanism. It is found that Ru species play a key role in activating carbonyl groups. This study illustrates a promising application of Ru/Nb_2O_5-Layer catalyst in the synthesis of amine and provides an understanding to the reaction mechanism.

Introduction

Amines are important compounds in natural products and medicines, and are irreplaceable intermediates in the synthesis of fine chemicals, including dyes, pesticide and herbicide.[1] Generally, there are three typical amination approaches: amination of halides, [2]hydrogen-borrowing amination of alcohol or phenol, [3]and the reductive amination of ketone or aldehyde.[4] The reaction from halides to amines has been well established.[1b] However, in this strategy some strict conditions are often required and the formation of the toxic and environmentally unfriendly by-products is also inevitable.[5] To overcome the drawbacks in this route, increasing attentions have been paid to the so-called 'hydrogen-borrowing amination'[6] and the reductive amination processes.[4] In the hydrogen-borrowing amination process, alcohols are used as the substrates and hydrogen resource as well. Typically, alcohols will directly react with ammonia after dehydrogenation, and the intermediates are then hydrogenated by the H_2 formed from the substrates.[7] As water is the only by-product during the reaction, this process is usually considered as a green process, but high reaction temperature (180~220 °C) is essential to achieve a good performance when heterogeneous catalysts are used in this strategy. The most practical and convenient approach for the synthesis of primary amines under mild conditions is the catalytic reductive amination of carbonyl compounds with ammonia and hydrogen. Up to now, many efforts have been made to the development of homogeneous catalysts for the selective preparation of primary amines by reductive amination.[8] Meanwhile, increasing attention has been attracted to the exploration of novel and high active heterogeneous catalysts in this area, as these kinds of catalysts show great commercial potential from an industrial view.[8a, 9] Very recently, Hara reported a high selective reductive amination of various aromatic carbonyl compounds over Ru/Nb_2O_5 catalysts and attributed the excellent performance to the weak electron-donating Ru on Nb_2O_5 surfaces.[10] They also suggested that the morphology of Ru species and the properties of Nb-based supports can strongly affect the reductive amination of furfural in their latest reports.[11]Therefore, it is believed that Ru/Nb_2O_5 catalytic system could be promising for the selective synthesis of primary amines from carbonyl compounds.

Cyclopentylamine (CPA) is an important fine chemical widely used as the ingredient in the manufacture of cosmetics, pesticides and medicines. Benefitting from the rapid development of biorefinery, the new route of CPA synthesis from biomass-derived cyclopentanone becomes promising. Cyclopentanone (CPO) is an important biomass-based platform compound and can be produced from furfural.[12] During the reductive amination of CPO, some side-reactions, such as over-hydrogenation, [9c] self-coupling of ketones and amines, [10] and Aldol condensation, [12] would be accompanied, so the high selective production of cyclopentylamine is a big challenge.

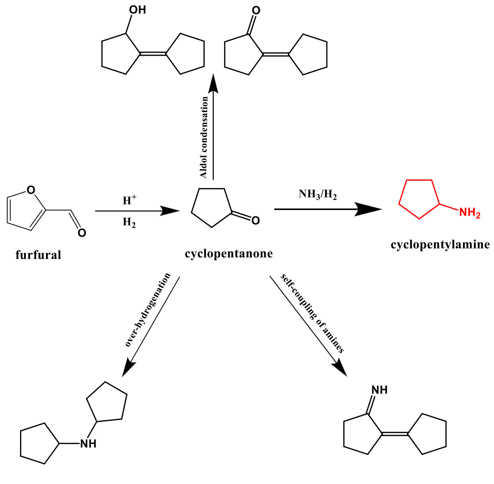

Scheme 1. Amination of cyclopentanone and accompanied by-reactions.

---

[a] W. J. Guo, T. Tao, Y. Guo, X.H. Liu, Prof. Y.Q. Wang
Shanghai Key Laboratory of Functional Materials Chemistry and Research Institute of Industrial Catalysis
School of Chemistry and Molecular Engineering, East China University of Science and Technology
No. 130 Meilong Road, Shanghai, 200237 (P.R. China)
E-mail: wangyanqin@ecust.edu.cn

⊥ These two authors contribute equally.

Supporting information for this article is given via a link at the end of the document.

Herein, Ru species supported on three kinds of niobium oxide (Nb_2O_5) with different morphology was studied for the reductive amination of cyclopentanone to cyclopentanylamine. The comprehensive structure-properties relationship was investigated through XPS, CO-titration and DRIFT-MS techniques. It is found that layered niobium oxide (Nb_2O_5-L) supported Ru catalyst has the best performance and it's the size of Ru, not the electronic properties influenced the activity. Moreover, the Ru/Nb_2O_5-L catalytic system shows a good durability and can be expanded to a series of aldehyde/ketone compounds, which suggest this system has a bright potential in industrial application.

Results and Discussion

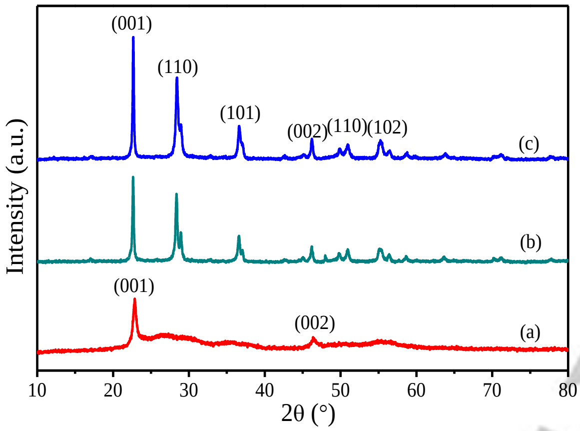

Figure 1. XRD patterns of Ru/Nb_2O_5 samples (a) 1%Ru/Nb_2O_5-L, (b) 1%Ru/Nb_2O_5-H, (c) 1%Ru/Nb_2O_5-F.

The XRD patterns present in Figure 1 show that both Ru/Nb_2O_5-F and Ru/Nb_2O_5-H catalysts have the characters of T-phase niobium oxide (JCPDS card no. 28-0317). The Ru/Nb_2O_5-L shows only two diffraction peaks at 22.7° and 46.2° obviously, indicating its layered structure and low degree of crystallinity.[13] It is need mentioned that no Ru diffraction peaks observed in all three catalyst, probably due to the low Ru loading (1 wt.%) or the good dispersion of Ru species over the niobium-based supports.

The morphologies of these three Ru/Nb_2O_5 samples were observed by TEM images and found that 1%Ru/Nb_2O_5-L has the rod-shaped morphology (Figure 2a), the 1%Ru/Nb_2O_5-H catalyst has spherical morphology, which may be accumulated by small Nb_2O_5 nanoparticles (Figure 2b) and the 1%Ru/Nb_2O_5-F shows a nanoslice-like morphology and assembled to nanoflower-like morphology when we observed in a large scale (under FE-SEM), which is in line with the previous report (Figure S1).[14] However, it is hard to destinguish the Ru particles in TEM images, due to the extremely small Ru particle size, which is in agreement with XRD results.

The Nitrogen sorption was carried out to measure the surface areas of all Ru/Nb_2O_5 catalysts, the data were summarized in Table 1. It is found that Ru/Nb_2O_5-L had the highest surface area (203 $m^2 \cdot g^{-1}$), followed with Ru/ Nb_2O_5-H (42 $m^2 \cdot g^{-1}$) and Ru/Nb_2O_5-F had the lowest (16 $m^2 \cdot g^{-1}$).

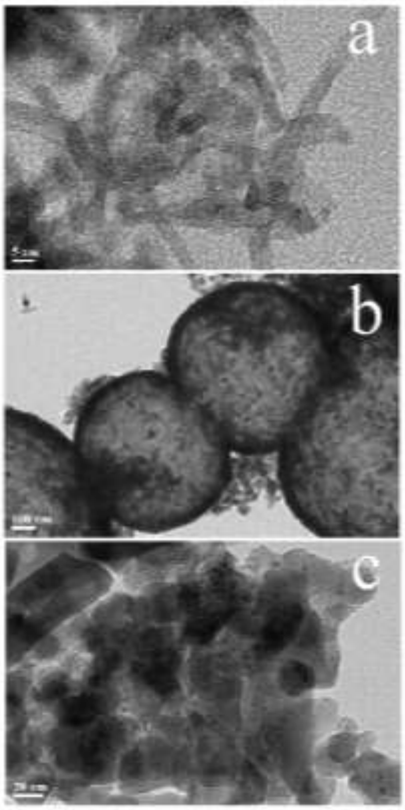

Figure 2. TEM images of (a) 1%Ru/Nb_2O_5-L, (b)1%Ru/ Nb_2O_5-H, and (c) 1%Ru/Nb_2O_5-F.

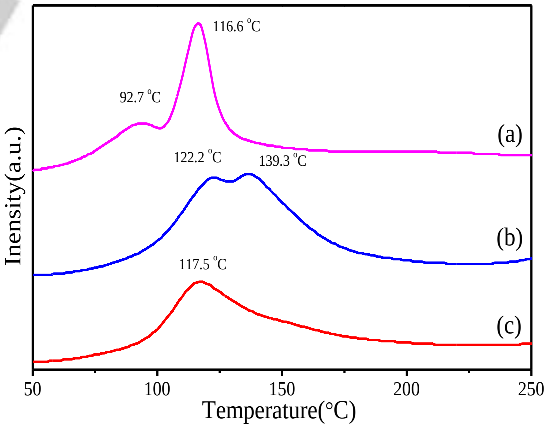

Figure 3. H_2-TPR profile of Ru/Nb_2O_5 catalysts (a) 1%Ru/Nb_2O_5-L, (b) 1%Ru/Nb_2O_5-H, (c) 1%Ru/Nb_2O_5-F.

NH_3-TPD analyses were also carried out to determine the surface acidity over all Ru loaded and pristine Nb_2O_5 samples (Figure.S5 and S6). Among all three Nb_2O_5 supports, Nb_2O_5-L possesses the largest acidity and Nb_2O_5-H has the lowest. After loading with Ru, the total acid amount changed, but the trend of acidity remains the same as that over pristine Nb_2O_5 samples.

Table 1. Yield of each product of CPO conversion over various catalysts[a]

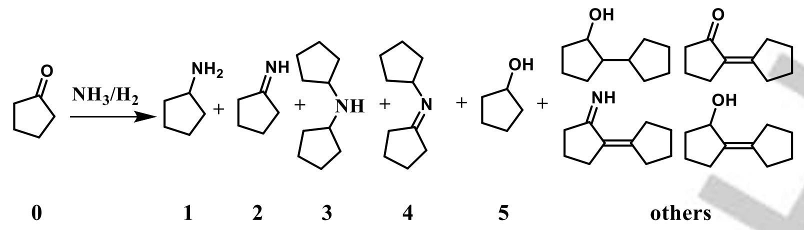

Catalysts	S_{BET} (m^2g^{-1})	Ru content (wt.%)	d[b] (nm)	D[c] (%)	Conv. (%)	Yield (%) 1	2	3	4	5	others	TOF[d] (min^{-1})
1%Ru/Nb_2O_5-L	203	0.98	1.8	76	100	84.3	0	4.1	1.0	9.1	1.0	58
1% Ru/Nb_2O_5-H	42	0.97	2.3	58	94.6	23.2	0	5.0	48.6	2.4	5.9	56
1% Ru/Nb_2O_5-F	16	0.96	8.4	16	73.5	0	3.3	0	35.7	2.0	16.7	57

[a] Condition: 2 mmol CPO,5 ml NH_3-MeOH(2M),20 mg catalyst, 90 ºC, 2 MPa H_2, 4 h; [b] Ru size(d) calculated by the dispersion of Ru ; [11] [c] Ru dispersion (D) determined by CO chemisorption; [d] The TOF value is calculated at ca. 20% conversion

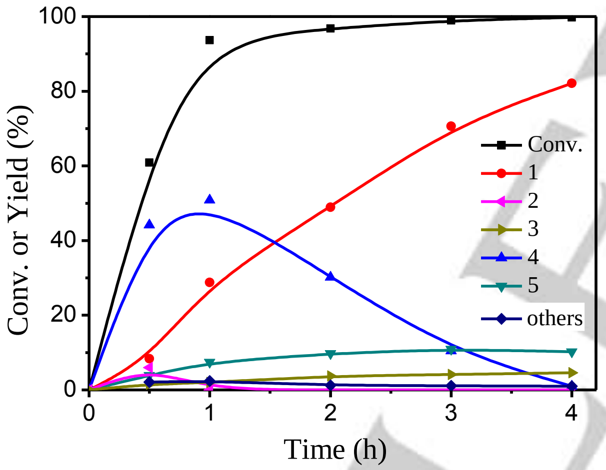

Figure 4. Effect of reaction time on the yield of products of cyclopentanone conversion

H_2 temperature-programmed reduction analysis (H_2-TPR) was introduced to compare the interaction between Ru species and Nb_2O_5 supports (Figure 3). All the samples show broad peaks in the range of 75-175 ºC and Ru/Nb_2O_5-L, Ru/Nb_2O_5-H and Ru/Nb_2O_5-F have a strong reduction peak at 116 °C, 122 ºC, and 117 ºC, respectively. In addition, a peak at 139 ºC is observed in the case of 1%Ru/Nb_2O_5-H, which may be caused by the stronger interaction between Ru species and Nb_2O_5-H support. Interestingly, a weak reduction peak appears at 92.7 ºC over 1%Ru/Nb_2O_5-L, which hints that Ru species may have a better dispersion on Nb_2O_5-L, this can be further confirmed by CO-titration results (Table 1) and will be discussed later.

.

After gaining the morphology and surface properties of these three 1%Ru/Nb_2O_5 catalysts, we then turned to compare their catalytic performance in the reductive amination of CPO, and the results are summarized in Table 1. It is obvious that 1%Ru/Nb_2O_5-L shows the best activity under the investigated conditions (90 ºC, 2 MPa H_2, 4 h) and the CPA yield reaches 84% with CPO completely converted. While, both 1%Ru/Nb_2O_5-H and 1%Ru/Nb_2O_5-F catalysts cannot convert all CPO within 4 hours, and a large amount of secondary imine (**4**, intermediate) remained in the catalytic system. What's worse is that no targeted product (CPA) was obtained over 1%Ru/Nb_2O_5-F during the test.

Reaction time courses were collected to investigate the reaction pathways (Figure 4) over 1%Ru/Nb_2O_5-L catalyst. It is found that imine (2) is generated at the very beginning of the reaction, and then rapidly hydrogenated to CPA. However, due to the higher nucleophilicity of CPA (compared with that of molecular ammonia), [15] part of CPA can react with CPO and forms the intermediate 4. When the reaction time was further prolonged, the amount of the secondary imine (4) decreased gradually with the yield of CPA increased. This suggests that intermediate **4** can be ammonolyzed to CPA under the co-existence of H_2 and NH_3. However, there is competitive hydrogenation of **4** to the secondary amine (**3**) and this process is irreversible. Therefore, the secondary amine (**3**) is the major by-product. In addition, a small amount of cyclopentanol was also detected, which comes from the direct hydrogenation of CPO. Besides these reactions, the aldol condensation of CPO also happens during this process, and the structures of these by-products (Figure 4, others) are verified by MS spectra (Figure S13-14). From above analysis, the whole reaction network can be clearly identified, which is summarized in Scheme 2.

The effect of reaction temperature and initial H_2 pressure was also investigated to find out the optimum conditions for this reaction, and the results are shown in Figure 5. Increasing either reaction temperature or H_2 pressure can accelerate the reaction rate. Clearly, the CPA yield rises steadily in the investigated period, while the yield of intermediate **4** continuously declines with the rising of reaction temperature or initial H_2 pressure. To balance the cost and productivity, the optimized operation conditions can be set at 90 °C and 2 MPa H_2 pressure.

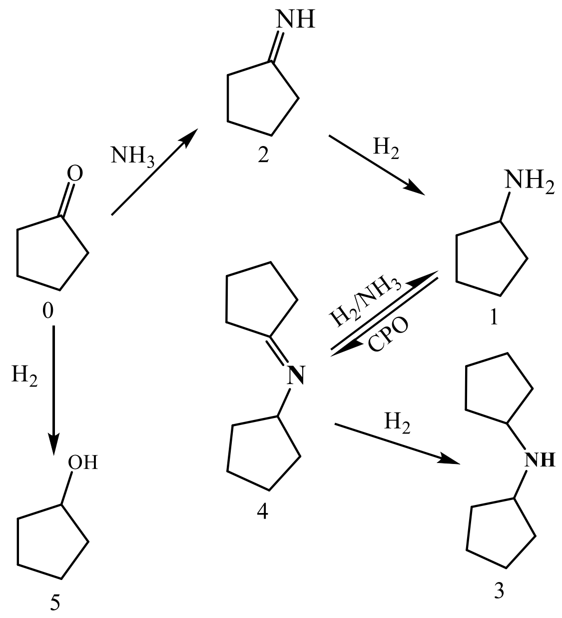

Scheme 2. Reaction pathways according to the time courses.

Recently, the chemical states of supported metals have been found to play an important role on the catalytic activity and selectivity in a wide range of reactions.[10, 15] Considering the previous report that the suitable chemical state of Ru species over Nb-based materials may have the promotional effect in reductive amination, [10] we measured the Ru states first in these three catalysts.

The XPS analyses of Ru $3d_{5/2}$ orbit of all three reduced 1%Ru/Nb_2O_5 catalysts were conducted (Figure 6). Ru species can be divided into two categories in all three catalysts, which can be associated to Ru^0 species at ca. 280.4 eV and $Ru^{\delta+}$ species at around 281.0 eV, respectively.[16] It can be found that the differences of Ru states over these three catalysts were not obvious.

Furthermore, the CO-adsorption DRIFT spectra were recorded to confirm the chemical states of Ru again over the three catalysts (Figure 7). Three bands can be clearly distinguished in all three spectra: the first band at the centre of 2014–2017 cm^{-1} can be assigned to the linearly adsorbed CO on Ru^0 species [Ru^0-CO]; the peak of the linearly adsorbed CO on partially oxidized $Ru^{\delta+}$ appears at 2077-2080 cm^{-1} [Ru^{n+}-CO]; and a tiny band centred at 2133-2141 cm^{-1} , which is usually considered to be the signal of tricarbonyl species on partially oxidized Ru [Ru^{n+}-$(CO)_3$].[16] Again, we didnot find significant difference of the location of CO over Ru species in all three catalysts, in consistence with XPS results.

Based on the results and discussions above, we can now rule out the possibility that the differences of catalytic performances for CPO reductive amination over the three catalysts are caused by the electronic effect of Ru species.

Since the electronic states of Ru species are identical in all these Ru/Nb_2O_5 catalysts, we turn to consider the geometric effect in the reaction. The H_2-TPR results show that the Ru dispersion over Nb_2O_5-L support are much higher than those of the rest two, so CO-pulse chemisorption was carried out to determine the dispersion of Ru particles and the data were added in Table 1.

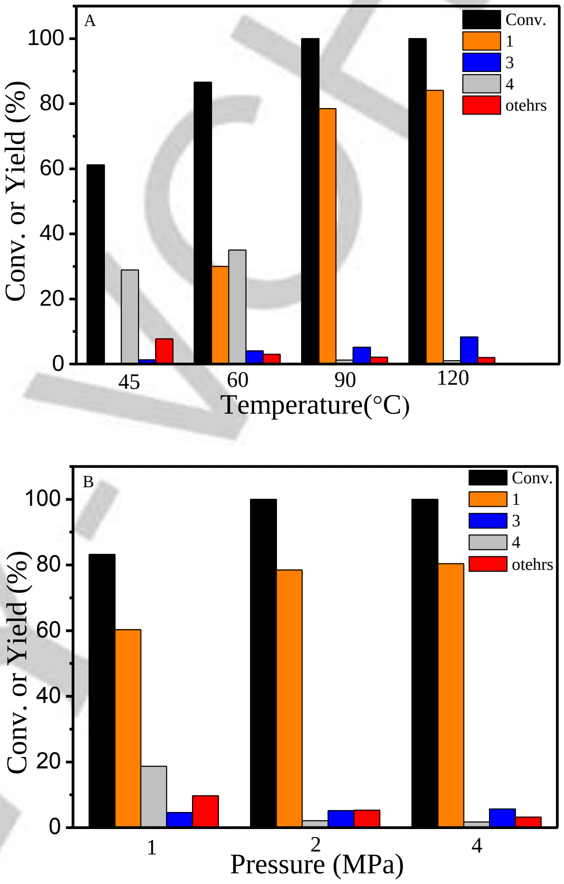

Figure 5. Effect of temperature and pressure on the conversion of CPO、Condition: (A) 2 mmol CPO,5 ml NH_3-MeOH (2 M),20mg 1%Ru/Nb_2O_5, 4 h, 2 MPa H_2. (B) 2 mmol CPO, 5 ml NH_3-MeOH (2 M), 20 mg 1% Ru/Nb_2O_5, 90 °C, 4 h.

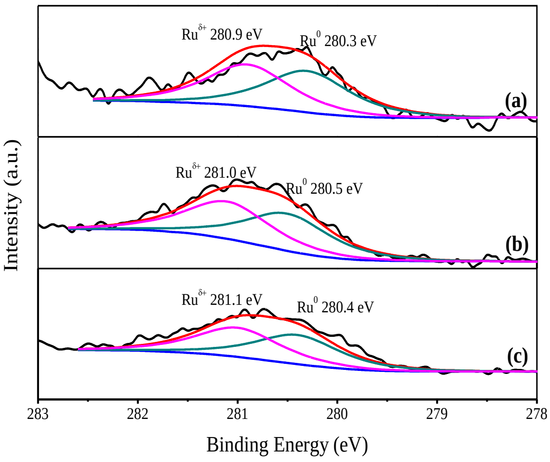

Figure 6. XPS spectra of Ru $3d_{5/2}$ for (a) 1%Ru/Nb_2O_5-L, (b) 1%Ru/Nb_2O_5-H, (c) 1%Ru/Nb_2O_5-F.

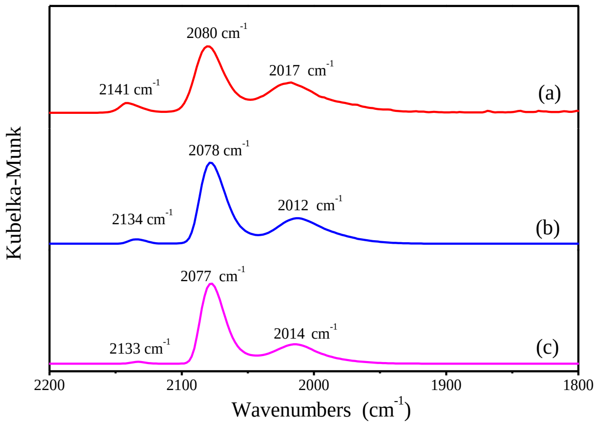

Figure 7. CO-adsorption DRIFT spectra at 25 °C over (a) 1%Ru/Nb_2O_5-L, (b) 1%Ru/Nb_2O_5-H, (c) 1%Ru/Nb_2O_5-F.

Obviously, Ru dispersion increases with the increase of the support's surface areas, and 1%Ru/Nb_2O_5-L possesses the largest dispersion of 76%. This result points out that under the premise of the identical Ru chemical states, a higher Ru dispersion is beneficial to the CPO reductive amination process. Moreover, the TOF values were calculated at lower conversion (ca. 20%) and added in Table1. It is found that the three data are similar, further confirming the key role of Ru partlcle size.

In addition, when we further analyzed the reaction result over 1%Ru/Nb_2O_5-F, it can be seen that besides its low activity, a large amount of condensed by-products is formed. This is basically caused by the low hydrogenation activity of 1%Ru/Nb_2O_5-F, whose dispersion is the lowest among all three catalysts. Namely, the competative side-reactions (mainly the Aldol condensation reaction) dominate the reaction, which are taking place over the acidic sites. This result again illustrates the importance of the high Ru dispersion in CPO reductive amination process.

Ru colloid (1.2 nm) was also prepared and loaded on various Nb_2O_5 to further clarify the role of Ru and support. It is found that Ru-colloid loaded Nb_2O_5 catalysts exhibit a slight difference in the catalytic performances (Table S2), compared to the remarkable differences over Ru-impregnated catalysts. This again highlights the decisive role of high Ru dispersion in CPO reductive amination.

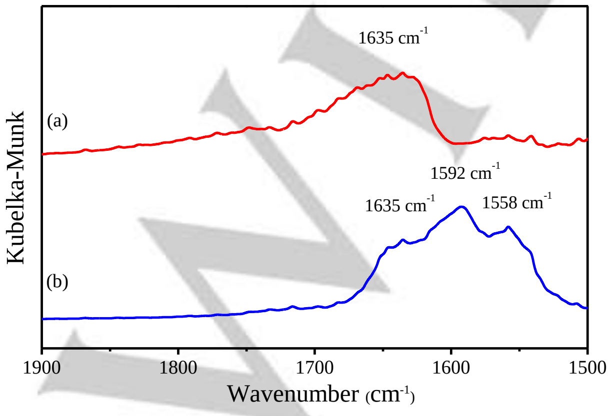

Figure 8. CPO-adsorption DRIFT spectra over (a) Nb_2O_5-L, (b) 1%Ru/Nb_2O_5-L.

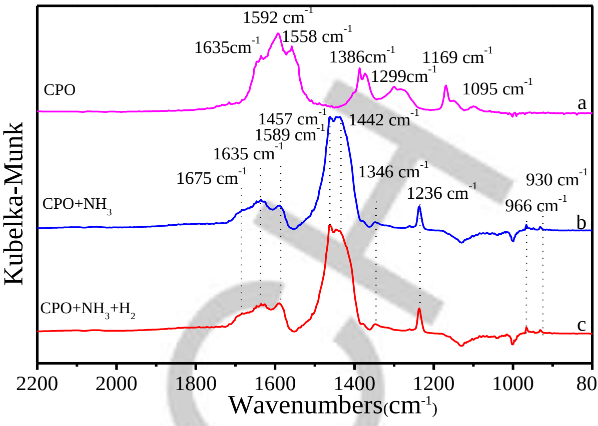

Figure 9. In situ DRIFT spectra for adsorption of (a) CPO, (b) CPO and NH_3, (c) CPO, NH_3 and H_2 on Ru/Nb_2O_5-L

To investigate the mechanism of the reaction and identify the active sites in the Ru-Nb systems, we conducted a series of DRIFT-MS experiments. The CPO-adsorption DRIFT spectra (Figure 8) over Nb_2O_5-L and 1%Ru/Nb_2O_5-L were collected, respectively. It can be seen only one broad band at ca. 1635 cm^{-1} appeared in the spectrum of Nb_2O_5-L, which can be assigned to the coordination of carbonyl group of CPO with L-acid sites.[17] In the case of 1%Ru/Nb_2O_5-L, the broad peak at around 1635 cm^{-1} still exists, suggesting that CPO is indeed adsorbed on the support. However, two new peaks at 1592 cm^{-1} and 1558 cm^{-1} appear in the spectrum of 1%Ru/Nb_2O_5-L. The former one can be assigned to the carbonyl group in CPO adsorbed on the surface of Ru particles, and the latter one can be considered as the carbonyl group of the aldol condensed by-products (Figure 5a, **others**) coordinated to L-acid sites. [17] The wavenumber of C=O groups shows an approximately 40 cm^{-1} red-shift over Ru species than that over the pristine Nb_2O_5 support, demonstrating that Ru species show a stronger ability to activate the C=O group. Thus, besides the function of H_2 activation, the Ru species can also act as active sites for the activation of carbonyl compounds during the reaction.

From the view of mechanism, the lone paired electrons in NH_3 molecule firstly undergoes nucleophilic attack with the C=O group of CPO to get the imine **2** during the CPO reductive amination reaction, [18] and then the intermediate **2** is further hydrogenated to the CPA. Since the C=O bond can be activated over the Ru/Nb_2O_5 catalyst, the behaviour of NH_3 over the catalysts should also be concerned. As the activated C=O bond can directly react with NH_3 through nucleophilic attack, the reaction may undergo via an Eley-Rideal (E-R) mechanism. We then used the in-situ DRIFT-MS technique to follow the surface reactions and explore the surface reaction mode during the CPO reductive amination over 1%Ru/Nb_2O_5-L catalyst.

After the adsorption of CPO (Figure 9 a), 30 mL NH_3 was pulsed into the chamber (Figure 9 b), and then changed to 5% H_2/Ar after 5-minute sweeping in Ar (Figure 9 c). The spectra of the latter two steps are of high similarity, and both show the typical characters of CPA and the reductive amination products of Aldol condensed by-product (Figure S4b and Table S1). This phenomenon seems so strange that since no molecular H_2 was introduced in the second step of our DRIFT-MS experiment,

Table 2 Conversion of different aldehydes and ketones over the 1%Ru/Nb_2O_5-L catalyst

Entry	Substrate	Time (h)	Product	Yield (%)
1	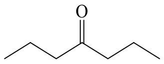	6	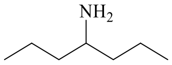	78
2	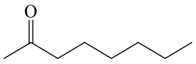	6	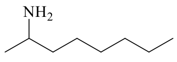	76
3	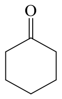	4	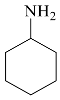	90
4	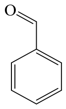	5	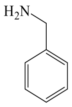	78
5	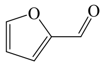	8	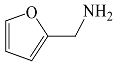	60
6	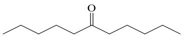	8	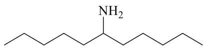	77

Condition: 2 mmol CPO, 5 mL NH_3-MeOH (2 M), 20 mg 1%Ru/Nb_2O_5-L, 90 °C, 2 MPa H_2

the production of CPA in this stage is totally unexpected. Surprisingly, when we analyzed the MS signal (Figure S2) during the reaction, it obviously showed that the ammonia molecules decompose to H_2 and N_2 over 1%Ru/Nb_2O_5-L, which is believed to be easy to occur over the Ru contented catalysts. [19] Consequently, it can now be expected that the formed H_2 immediately hydrogenates the intermediate **2** to CPA (**1**); as a result, no signal of **2** was detected. This finding suggests that the activation of NH_3 over Ru species is unnecessary for the reductive amination and the adsorption of ammonia over Ru sites can cause the NH_3-deposition side-reaction, declining the ultilisation of ammonia. Also, a large amount of NH_3 was found to be adsorbed on the B-acid and L-acid sites (1457 cm^{-1} and 1675 cm^{-1} respectively，see Figure S4a and Table S1) over 1%Ru/Nb_2O_5 catalyst, and the adsorbed NH_4^+ and NH_3→L species are usually regarded to be inactive during the reductive amination of ketones/aldehydes, as they have no ability to share the paired electrons. In brief, the in situ DRIFT-MS data infer that the ammonia molecule is more likely to directly react with the Ru-adsorbed CPO over the surface of catalysts, which follows an Eley-Rideal (E-R) mechanism.[20]

Durability test and substrate scope over 1%Ru/Nb_2O_5-L catalyst

The durability of the catalytic systems is one of the most important properties concerned in the industry, so the recycling tests were conducted to see the stability of the 1%Ru/Nb_2O_5-L catalyst. Figure 10 clearly shows that no significant decrease in activity or selectivity was observed during the initial three successive runs and only a tiny decline of the catalytic performance was seen in the 4th and 5th runs, which illustrates the good stability of the catalytic system. Also, the XRD (Figure S3) and ICP-AES results of the spent catalyst were also recorded. These results show that neither the phase composition nor Ru content of the spent catalyst (0.9 wt.%) show remarkable changes, compared with the fresh one. Then, the 1%Ru/Nb_2O_5-L catalyst was further applied to a wide range of aldehydes and ketones, including long-chain ketones, cyclic ketone and aromatic aldehyde (Table 2). The results show that this system is suitable to all investigated substrates and a high yield of primary amines can be achieved.The good stability of 1%Ru/Nb_2O_5-L and its excellent compatibility in the conversion of different substrates highlight this system's bright future in the amine-production.

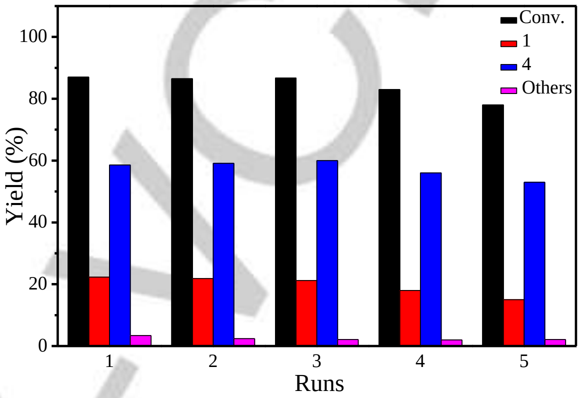

Figgure 10. The durability test of 1%Ru/Nb_2O_5-L catalysts.
Condition: 2 mmol CPO, 5 mL NH_3-MeOH (2 M), 20 mg Catalysis, 90 °C, 2 MPa H_2, 1 h.

Conclusions

In summary, we successfully synthesis three 1%Ru/Nb_2O_5 catalysts with different morphologies for a comparative investigation in the reductive amination of cyclopentanone, and the best catalytic performance can be achieved over 1%Ru/Nb_2O_5-L (a CPA yield of 84%). Furthermore, 1%Ru/Nb_2O_5-L catalyst shows good stability during CPO reductive amination process, and can successfully be expanded to a series of substrates to produce the corresponding primary amines. Our results manifest that the activity of the reaction systems is mainly controlled by the geometric effect of Ru particles when the chemical states of Ru are identical. Nb_2O_5 supports (like Nb_2O_5-L material) with higher specific area are able to promote the dispersion of active Ru species over the surface of catalysts. Importantly, good Ru dispersion of catalysts can enhance the hydrogenation capability during this reaction, and thus can suppress the acid-related side-reaction over Nb-based supports. Our DRIFT-MS data illustrate that Ru species activate the carbonyl groups and H_2 during the reaction, and the reaction between aldehyde/ketone species and ammonia is considered to undergo via an E-R mechanism. This study provides an in-depth understanding of surface processes during the reaction and firmly points out that our 1%Ru/Nb_2O_5-L catalyst can be one of the promising candidates for green aldehyde/ketone reductive amination process.

Experimental Section

Catalyst preparation

The Layer Nb_2O_5 (labeled as Nb_2O_5-L) was prepared by a modified hydrothermal method.[13] Typically, 19.2 g self-synthesized niobium oxalate solution (0.5 mol/L) and 0.71 g ammonium oxalate were well mixed in 40 mL deionized water, and then transferred to a 100 mL Teflon-lined stainless-steel autoclave. After the autoclave was steeled, the mixed solution was kept under 180 °C for 3 days. Then, the white powder was collected by filtration, followed by drying at 100 °C for 12 h, and calcined at 400 °C for 4 h in air. The hollow Nb_2O_5 (labeled as Nb_2O_5-H) was fabricated through a modified one-pot hydrothermal method according to the literature.[21] In a typical process, 1.368 g of resorcinol (R) 2.016 g of formaldehyde and 9.6 g of niobium oxalate aqueous solutions were mixed in 50 mL DI water at room temperature. After stirring for 4 h at 40 ºC, the solution was transferred to a 100 mL Teflon-lined autoclave, and heated at 180 ºC for 24 h. The resulting precipitates were collected, filtered, washed with DI-water several times, then dried at 60 ºC for 24 h and calcined at 600 °C (2 ºC·min^{-1}) for 2 h in air. Flower-like Nb_2O_5 (labeled as Nb_2O_5-F) were also synthesized via a modified hydrothermal process according to literature.[14] In a typical synthesis process, 0.4 g $NbCl_5$ was dissolved in 4 ml ethanol. Then, 17 ml deionized water and 3 ml ammonium hydroxide solution were added into the $NbCl_5$ ethanol solution under vigorous stirring, and the mixture was stirred for another 2 h at room temperature. Then the white precipitates were separated by centrifugation and ultrasonically re-dispersed in 56 ml DI water. The suspension was transferred and sealed into a 100 mL Teflon-lined autoclave, and heated at 200 ºC for 24 h. The resulting precipitates were collected, filtered, washed with DI-water three times, then dried at 60 ºC for 24 h and calcined at 400 °C (2 ºC·min^{-1}) for 2 h in air to obtain Nb_2O_5-F.

All Ru/Nb_2O_5 catalysts were prepared by incipient wetness impregnation method. Typically, a certain amount of 10 wt.% $RuCl_3$ aqueous solution was added to the Nb_2O_5 supports and stirred to be a slurry. Then the slurry was dried at 60 °C for 12 h, and 110 °C for another 12 h. Before used, the catalysts were reduced at 400 °C for 2 h under 10% H_2-Ar mixed gas. The catalysts prepared were labeled as Ru/Nb_2O_5-n (n = L, H, F), respectively, depending on the Nb_2O_5 support used. The initial content of Ru is fixed at 1 wt.% and the final content was measured by an Agilent 725ES inductively coupled plasma atomic emission spectrometry (ICP-AES), which is very close to the initial one (Table 1).

The Ru-colloid loaded Nb-based catalysts with the same Ru particles were prepared by adsorption of colloidal Ru nanoparticles (NPs) onto the Nb_2O_5-L, Nb_2O_5-H and Nb_2O_5-F supports.[22] Colloidal Ru NPs with size of 1.2 nm was prepared through the reduction of $RuCl_3$ with ascorbic acid in the aqueous phase 80 ºC for 1 min. Then, add the support into the colloidal Ru particle solution and stirred for 24 h. Finally, it was washed by DI water and dried at 50 ºC vacuum oven. Before used, it was solidified at 300 ºC for 4 h under a N_2 flow. The content of Ru NPs was 1.0 wt %.

Catalysts activity tests

The reductive amination of CPO was conducted in a Teflon-lined stainless-steel autoclave (50 mL). After sealing the desired dosage of CPO, catalyst, and NH_3-CH_3OH solution (2M) in the reactor, the autoclave was purged with H_2 three times and pressurized to the desired pressure. Then, the autoclave was heated to the predetermined temperature in a short time. After reaction, the reactor was quenched in an ice-water bath immediately.

The liquid phase was separated from the catalyst by centrifugation, and two individual GC/GC-MS systems were used for product analyses. The qualitative analysis of products was carried out on a GC-MS system (Agilent 7890A-5975C), and the quantitative analysis was executed on a GC system (Agilent 7890B) equipped with an HP-5 column and an FID detector.

The TOF value of CPO reductive amination is calculated by the following equation:

$$TOF = \frac{Conv.(\%) \times (n_{CPO} / n_{Ru})}{time(min) \times D_{Ru}}$$

Catalyst characterization

All synthesized Ru/Nb_2O_5 catalysts were extensively characterized to understand the structure-property relationships of the catalytic system.

Powder X-ray diffraction (XRD) patterns were recorded in the θ-2θ mode on a D8 Focus diffractometer (CuKα1 radiation, k = 1.5406 Å), operated at 40 kV and 40 mA within scattering angels of 10-80°. Nitrogen sorption measurements were performed on a Micromeritics ASAP 2020 sorption analyzer. The samples were degassed at 200 °C for 6 h, and measured at -196 ºC. The Brunauer-Emmett-Teller (BET) method was adopted to calculate the specific surface area. Scanning electron microscopy (SEM) was recorded on a Nova NanoSEM 450 microscopy at 3 kV. Transmission electron microscopy (TEM) was obtained on a JEOL Model 2100 electron microscopy at 200 kV. Hydrogen temperature-programmed-reduction (H_2-TPD) was carried out in a PX200 apparatus with a thermal conductivity detector (TCD).

The Ru dispersion was measured by CO chemisorption using the dynamic adsorption method with an automatic chemisorbent (ChemiSorb 2720). Before adsorption, the sample (0.1 g) was reduced at 200 ° C for 30 min (10 °C/min) under pure H_2 (60 mL/min), cooled to room temperature, and flushed in He for 30 minutes. Then, a pulse of 5% CO in He was injected through a thermal conductivity detector (TCD) until saturation was reached. Ru dispersion was calculated by assuming that the stoichiometric ratio of CO adsorbed by Ru is 1:1.

Ammonia temperature-programmed-desorption (NH_3-TPD) was carried out in a PX200 apparatus (Tianjin Golden Eagle Technology Limited Corporation) with a thermal conductivity detector (TCD). The sample (50 mg) was charged into a quartz reactor, and the temperature was raised from room temperature to 600 ºC at a rate of 10 ºC min -1 under a flow of N_2 (50 ml min^{-1}), and then the temperature was cooled to 90 ºC. Then, the NH_3 (5 ml min^{-1}) was injected into the reactor at 90 ºC under a flow of N_2 (45 ml min^{-1}). When the adsorption saturation is reached, the N_2 (25 ml min^{-1}) is flowed at 90 ºC for 1 hour, then the temperature is raised from 90 ºC to 600 ºC （10 ° C min^{-1}） and the amount of ammonia was detected at 110 ºC by using a thermal conductivity detector(TCD).

X-ray photoelectron spectroscopy (XPS) spectra were recorded on a Thermo Scientific Escalab 250 Xi system with monochromatic Al Kα radiation, and the results were calibrated using the C 1s peak at 284.6 eV. Diffuse reflectance infrared Fourier transform spectra (DRIFTS) were recorded on a Nicolet Model iS-50 FT-IR spectrometer equipped with an MCT/A detector, and the sample cell was fitted with ZnSe windows. The DRIFT spectra of CO-adsorption (1% CO/Ar) were recorded with a resolution of 4 cm^{-1} and 32 scans at 30 ºC. DRIFT-MS spectra was also recorded on a Nicolet Model iS-50 FT-IR spectrometer which was same as DRIFT spectra. The samples were loaded onto DRIFT IR cell, then reduced at 400 °C for 1 h under 5% H_2-Ar mixed gas. After cooled to the 30 ºC, Ar (99.99% pure) was passed through a bubbler containing CPO via a volume flow controller before entering the DRIFT cell in 30 min，then flushed in Ar without CPO for 30 minutes. After that the NH_3 was pulsed into the DRIFT cell, and then changed to 5%H_2/Ar after 5-minute sweeping in Ar. The flow rate remained constant at 30 ml/min for all experiments. Collect infrared spectra after each gas exchange. The gaseous effluent from the reactor was monitored by a Mass Spectrometer (MS). The following m/z ratios were monitored on the LingLu Instruments QAS 100 mass spectrometer: 2 (H_2), 17(NH_3), 28 (N_2) and 40 (Ar).

Acknowledgements

This work was supported financially by the NSFC of China (No. 21832002, 21872050, 21808063), the Fundamental Research Funds for the Central Universities (222201718003) and the Science and Technology Commission of Shanghai Municipality (18ZR1408500, 10dz2220500).

Keywords: reduction amination• biomass• DRIFT-MS • niobium oxide• geometric effect

[1] a) V. Froidevaux, C. Negrell, S. Caillol, J.-P. Pascault, B. Boutevin, *Chem. Rev.* **2016**, *116*, 14181-14224; b) M. Pelckmans, T. Renders, S. Van de Vyver, B. F. Sels, *Green Chem.* **2017**, *19*, 5303-5331; c) K. S. Hayes, *Appl. Catal., A.* **2001**, *221*, 187-195; d) K.-i. Shimizu, K. Kon, W. Onodera, H. Yamazaki, J. N. Kondo, *ACS Catal.* **2013**, *3*, 112-117; e) J. P. Wolfe, H. Tomori, J. P. Sadighi, J. Yin, S. L. Buchwald, *J. Org. Chem.* **2000**, *65*, 1158-1174; f) M. S. Driver, J. F. Hartwig, *J. Am. Chem. Soc.* **1996**, *118*, 7217-7218.

[2] Z. Dong, G. Dong, *J. Am. Chem. Soc.* **2013**, *135*, 18350-18353.

[3] A. Said Stålsmeden, J. L. Belmonte Vázquez, K. van Weerdenburg, R. Rae, P.-O. Norrby, N. Kann, *ACS Sustainable Chem. Eng.* **2016**, *4*, 5730-5736.

[4] A. F. Abdel-Magid, K. G. Carson, B. D. Harris, C. A. Maryanoff, R. D. Shah, *J. Org. Chem.* **1996**, *61*, 3849-3862.

[5] H. Kim, S. Chang, *ACS Catal.* **2016**, *6*, 2341-2351.

[6] a) M. R. Ball, T. S. Wesley, K. R. Rivera-Dones, G. W. Huber, J. A. Dumesic, *Green Chem.* **2018**, *20*, 4695-4709; b) T. Cuypers, P. Tomkins, D. E. De Vos, *Catal. Sci. Technol.* **2018**, *8*, 2519-2523.

[7] M. H. S. A. Hamid, P. A. Slatford, J. M. J. Williams, *Adv. Synth. Catal.* **2007**, *349*, 1555-1575.

[8] a) T. Senthamarai, K. Murugesan, J. Schneidewind, N. V. Kalevaru, W. Baumann, H. Neumann, P. C. J. Kamer, M. Beller, R. V. Jagadeesh, *Nat. Commun.* **2018**, *9*, 4123; b) J. Gallardo-Donaire, M. Ernst, O. Trapp, T. Schaub, *Adv. Synth. Catal.* **2016**, *358*, 358-363; c) H. Huang, X. Liu, L. Zhou, M. Chang, X. Zhang, *Angew. Chem., Int. Ed.* **2016**, *55*, 5309-5312.

[9] a) G. Liang, A. Wang, L. Li, G. Xu, N. Yan, T. Zhang, *Angew. Chem., Int. Ed.* **2017**, *56*, 3050-3054; b) R. V. Jagadeesh, K. Murugesan, A. S. Alshammari, H. Neumann, M. M. Pohl, J. Radnik, M. Beller, *Science* **2017**, *358*, 326-+;M. Chatterjee, T. Ishizaka, H. Kawanami, *Green Chem.* **2016**, *18*, 487-496.

[10] T. Komanoya, T. Kinemura, Y. kita, K. Kamata, M. Hara, *J. Am. Chem. Soc.* **2017**, *139*, 11493-11499.

[11] a) D. Chandra, Y. Inoue, M. Sasase, M. Kitano, A. Bhaumik, K. Kamata, H. Hosono, M. Hara, *Chem. Sci.* **2018**, *9*, 5949-5956; b) D. Deng, Y. Kita, K. Kamata, M. Hara, *ACS Sustainable Chem. Eng.* **2018**.

[12] Y. L. Yang, Z. T. Du, Y. Z. Huang, F. Lu, F. Wang, J. Gao, J. Xu, *Green Chem.* **2013**, *15*, 1932-1940.

[13] T. Murayama, J. Chen, J. Hirata, K. Matsumoto, W. Ueda, *Catal. Sci. Technol.* **2014**, *4*, 4250-4257.

[14] W. Dong, F. Pan, Y. Wang, S. Xiao, K. Wu, G. Q. Xu, W. Chen, *Appl. Surf. Sci.* **2017**, *392*, 514-522.

[15] H. K. Hall, R. B. Bates, *Tetrahedron Lett.* **2012**, *53*, 1830-1832.

[16] a) S. Zhang, Z. Xia, T. Ni, Z. Zhang, Y. Ma, Y. Qu, *J. Catal.* **2018**, *359*, 101-111; b) T. Tong, X. Liu, Y. Guo, M. Norouzi Banis, Y. Hu, Y. Wang, *J. Catal.* **2018**, *365*, 420-428; c) S. Li, Y. Xu, Y. Chen, W. Li, L. Lin, M. Li, Y. Deng, X. Wang, B. Ge, C. Yang, S. Yao, J. Xie, Y. Li, X. Liu, D. Ma, *Angew. Chem., Int. Ed.* **2017**, *56*, 10761-10765.

[17] J. An, Y. Wang, J. Lu, J. Zhang, Z. Zhang, S. Xu, X. Liu, T. Zhang, M. Gocyla, M. Heggen, R. E. Dunin-Borkowski, P. Fornasiero, F. Wang, *J. Am. Chem. Soc.* **2018**, *140*, 4172-4181.

[18] M. I. Zaki, M. A. Hasan, L. Pasupulety, *Langmuir* **2001**, *17*, 768-774.

[19] S. F. Yin, B. Q. Xu, X. P. Zhou, C. T. Au, *Appl. Catal., A* **2004**, *277*, 1-9.

[20] J. Mai, W. von Niessen, *Chem. Phys.* **1991**, *156*, 63-69.

[21] L. Kong, C. Zhang, J. Wang, W. Qiao, L.Ling, D. Long, *Sci. Rep.* **2016**, 6, 21177.

[22] L. Dong, L.-L. Yin, Q. Xia, X. Liu, X.-Q. Gong, Y. Wang, *Catal. Sci. Technol.* **2018**, 8, 735-745.

Text for Table of Contents

Cyclopentylamine is high selectively obtained over layered Nb_2O_5 supported Ru catalyst by the reductive amination of cyclopentanone.

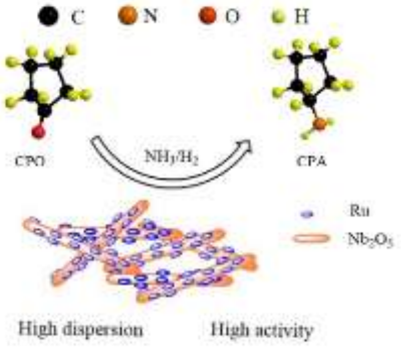

Wanjun Guo[⊥], *Tao Tong*[⊥], *Xiaohui Liu, Yong Guo, Yanqin Wang**

Page No. – Page No.

Morphology-tuned activity of $RuNb_2O_5$ catalysts for ketones reductive amination